ELSEVIER

The measurement of $\partial u/\partial y$ in a turbulent boundary layer over a riblet surface

Y. Dubief, L. Djenidi, and R. A. Antonia
Department of Mechanical Engineering, University of Newcastle, NSW Australia

Statistics of $\partial u/\partial y$ have been measured in a turbulent boundary layer over either a smooth wall or a riblet surface using parallel hot wires. Over the riblets, the mean square value of $\partial u/\partial y$ (normalised with smooth wall variables) is smaller than over the smooth wall; the difference increases as the distance to the wall decreases. Also this difference is larger when the riblets operate in a drag-augmenting mode. These changes would reflect changes in the near-wall turbulence structure. Furthermore, on the basis that $\partial u/\partial y$ is a major contributor to the spanwise vorticity, the results indicate that, relative to the smooth wall, the mean square spanwise vorticity is reduced near a riblet surface. © 1997 by Elsevier Science Inc.

Keywords: turbulent boundary layer; riblets; velocity derivative; hot wire measurements

Introduction

Measurements and direct numerical simulations (DNS) of a turbulent boundary layer over riblets (longitudinal wall grooves) have shown that skin frictional drag reduction is possible when s^+ and h^+ (s and h are the transverse separation and height, respectively, of the riblets; the superscript $^+$ denotes normalisation by wall variables) are smaller than about 20, the maximum reduction occurring when $s^+ \simeq 15$ (Walsh 1990). When $s^+ \geq 30$, the riblets tends to increase the skin frictional drag, by comparison to a smooth wall. Choi et al. (1993) suggested, on the basis of their DNS data, that drag reduction or drag augmentation are the direct result of interference between the riblets and the near-wall quasi-streamwise vortices. In particular, drag reduction followed when s^+ (or h^+) is comparable to the average size of the vortices. For larger values of s^+, the drag area of the riblets is exposed to the downwash of the high-speed flow that the vortices induce, and there is a corresponding increase in drag.

In the context of this explanation, it is clearly of interest to have data on all three vorticity components near the riblet wall. The DNS data (Choi et al. 1993) indicated a reduction in the local maximum of ω_x' (the prime denotes the rms value) when the riblets are in drag-reducing configuration ($s^+ = 20$); for $s^+ = 40$, all three rms vorticities are increased above the riblets. Choi et al. noted that there are no known experimental data on vorticity fluctuations above riblets. This is not surprising given the difficulty in obtaining reliable estimates of ω near a surface. Spatial resolution requirements preclude the use of a multiple wire three-component vorticity probe in this flow region. A one-component vorticity probe may be more suitable, but even then there is a need to make corrections due to the attenuation of the high wave number part of the spectrum. Corrections are based on local isotropy, an assumption which is not valid near a wall.

The approach followed in the present study is to measure the gradient $\partial u/\partial y$, a quantity which was estimated with relatively good accuracy in the wall region of a fully developed channel flow using parallel hot wires (Antonia et al. 1993). It should be noted that on a smooth wall $(\partial u/\partial y)'$ represents about 60% of ω_z' ($\omega_z = \partial v/\partial x - \partial u/\partial y$) in the outer region of the flow—this contribution increases in the inner region to reach 100% at the wall—(Antonia et al. 1991). We may expect that over riblets, $(\partial u/\partial y)'$ contributes significantly to ω_z'. In this paper, we present measurements of $\partial u/\partial y$ in a turbulent boundary layer over a riblet surface. By varying the free-stream velocity, measurements could be made for $s^+ = 17$ and $s^+ = 29$; i.e., drag-reducing and drag-augmenting conditions, over the same surface. The reference smooth wall values were obtained using the same probe and instrumentation by inserting a "dummy" smooth surface on top of the riblets.

Experimental details

The experiments were carried out in an open-return, suction-type wind tunnel, including a bell mouth inlet, a honeycomb section, a short settling chamber fitted with screens, and a 5:1 two-dimensional (2-D) contraction. The working section is 3.25-m long, 0.6-m wide, and 0.11-m high at the inlet. A 2-D diffuser and a transition section isolate the working section from any potential disturbances associated with the axial fan.

The boundary layer developed on the bottom wall of the working section after it was tripped by the combination of a 2-mm diameter cylinder and a 50-mm wide coarse grain sandpaper. The first 1m section of the wall was smooth. The next 1m consisted of the riblet surface: longitudinal triangular shaped grooves machined out of aluminium ($h = s = 2.5$ mm) cover the complete span of the working section (see Figure 1). The crest plane of the riblets was flush with the upstream smooth wall and the downstream (1.25-m long) smooth wall. For the "reference"

Address reprint requests to Prof. R. A. Antonia, Dept. of Mechanical Engineering, The University of Newcastle, University Drive, Callaghan, Newcastle, NSW 2308, Australia.

Received 6 March 1996; accepted 9 July 1996

Int. J. Heat and Fluid Flow 18: 183–187, 1997
© 1997 by Elsevier Science Inc.
655 Avenue of the Americas, New York, NY 10010

0142-727X/97/$17.00
PII S0142-727X(96)00091-0

smooth wall measurements, a 3-mm thick sheet of Laminex was placed over the riblet section. The sheet was maintained flat by taping it against the vertical walls of the working section. The leading edge ($x = 0.65$ m) of the sheet was tapered down to a thin wedge in order to minimise any disturbance at the measurement station ($x = 1.2$ m). The roof of the working section was adjusted to maintain a zero pressure gradient.

A single hot wire was used to measure $\overline{U}$ and u'. Parallel hot wires (sketched in Figure 1) were used for the measurements of $\partial u/\partial y$. All wires (Pt-10% Rh) had a diameter of 2.5 μm, a nominal length l of 0.5 mm and were operated at an overheat ratio of 1.5 with inhouse constant temperature circuits. The output signals were amplified, filtered, and digitized using a 16-channel, 12-bit A/D data-acquisition system (Boston technology) and stored in a 486 DX PC for subsequent data analysis. The cut-off frequency was about 2.5 kHz, and the sampling frequency was about 5 kHz at all position points. The probes were mounted on a height gauge and traversed into the free-stream velocity for calibration. The free-stream velocity U_1 was monitored continuously with a pitot-static tube connected to a MKS Baratron pressure transducer (see Antonia et al. 1994 for further details on the Baratron).

Results and discussion

Mean and fluctuating streamwise velocity

Before considering the measurements of $\partial u/\partial y$, it is important to ascertain the quality of the (single hot-wire) measurements of $\overline{U}$ and u. Figure 2 (a semilogarithmic scale is used) shows distributions of $\overline{U}$ and u' over smooth and riblet (crest and trough) surfaces for $R_\theta = 540$ ($s^+ = 17$) and $R_\theta = 940$ ($s^+ = 29$) [θ is the momentum thickness measured on the smooth wall, cf. Figure 1]. The smooth wall friction velocity U_τ used for normalising the data in Figure 2 and all subsequent figures, was obtained by assuming a power-law velocity distribution (Barenblatt 1993; Barenblatt and Prostokishin 1993). The numerical values of U_τ agreed with those inferred from the wall shear-stress measured with a Preston tube (Djenidi et al. 1996). The origin for the riblet velocity profiles is taken at the virtual origin—defined as the origin of the spanwise averaged velocity profiles (Bechert and Bartenwerfer 1989).

The present results compare generally well with available (not shown here) hot-wire (Vukoslavcevic et al. 1992; Park and Wallace 1994), LDA (Benhalilou et al. 1994; Djenidi and Antonia 1996) and DNS (Choi et al. 1993) data. For example, there is no spanwise variation in either $\overline{U^+}$ or $u^{+'}$ when y^+ is greater than about one riblet height above the riblet crest plane. Only in the region near the riblet wall is a spanwise variation discerned; in this region, the spanwise inhomogeneity of the wall geometry affects the flow through the action of viscosity. Because the data are normalised by the smooth wall friction velocity, neither the expected upward shift (drag reduction) nor downward shift (drag increase) in $\overline{U^+}$ relative to the smooth wall are evident in Figure 2a. Also consistent with the previously cited studies is the near-wall reduction of $u^{+'}$, relative to the smooth wall. The near-wall behaviour of the data when the riblets operate in a drag-increasing mode ($s^+ = 29$) is somewhat uncharacteristic. Earlier studies (see references cited above) clearly showed that in the near-wall region of a drag-augmenting riblet surface, $u^{+'}$ is larger over the crest than over the valley. This is not observed in the present data. Arguably, this behaviour can be attributed to the spanwise integration effect ($l^+ = 5.8$ when $s^+ = 29$) over a region where

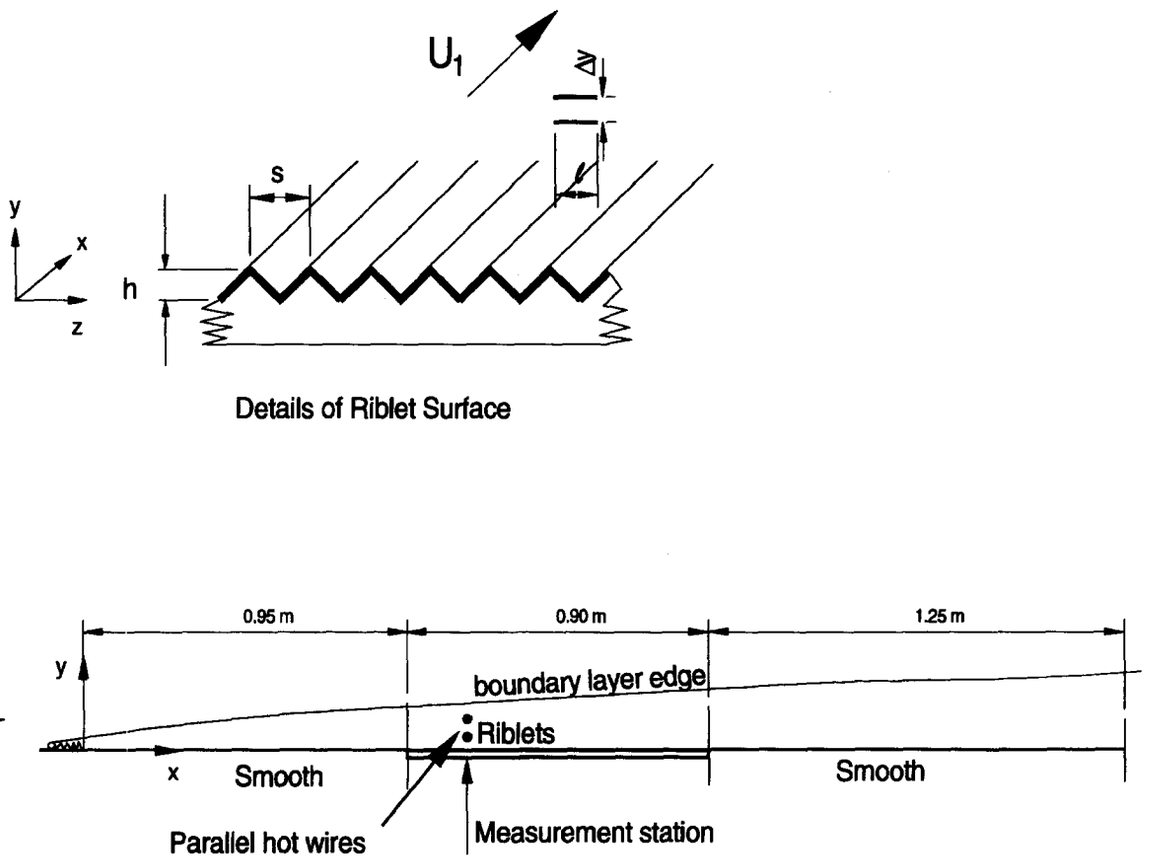

Figure 1 Layout of the working section bottom wall, showing the riblet surface and the parallel hot wires

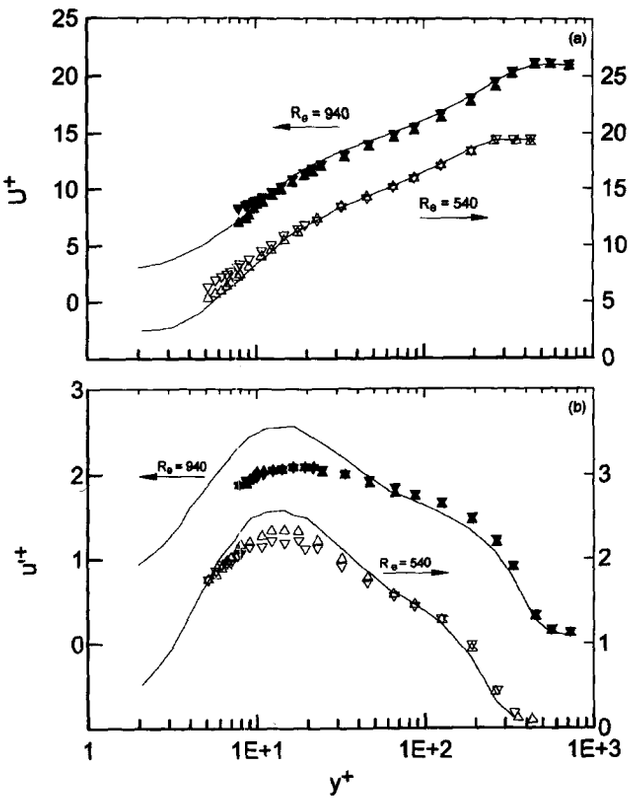

Figure 2 Mean (a) and rms (b) longitudinal velocity distributions over smooth and riblet surfaces; the origin of the riblet data is taken at the fictitious origin; —, smooth wall; symbols, riblet surface: ▲ (peak) and ▼ (valley), $s^+ = 29$; △ (peak) and ▽ (valley), $s^+ = 17$

mean velocity gradients in the spanwise direction are large. The spanwise variation in mean velocity is much larger near the crest than near the valley; this trend is particularly significant in planes parallel to the riblet crest plane. The lack of any perceptible difference between peak and valley may also be due to the riblet geometry used here ($s = h$).

$\partial u/\partial y$

Parallel hot wires, separated by a distance Δy in the wall-normal direction, can, in principle, allow statistics of $\partial u/\partial y$ to be inferred from those of the finite difference ratio $\Delta u/\Delta y$, where $\Delta u \equiv u(y+\Delta y) - u(y)$. However, the accuracy of the statistics depends critically on the selection of Δy. This selection is particularly delicate in the wall region, because corrections to the $\partial u/\partial y$ spectrum and therefore $\overline{(\partial u/\partial y)^2}$ rely on the assumption of local isotropy. An alternative approach is to use the two-point correlation method. The value of $\overline{(\partial u/\partial y)^2}$ is inferred from the expression

$$1 - R_{uu}(\Delta y) = (\Delta y)^2 \left[\frac{1}{2\overline{(u^2)}} \overline{(\partial u/\partial y)^2} - \frac{1}{8\overline{(u^2)}^2} \overline{(\partial u^2/\partial y)^2} \right] \quad (1)$$

which is obtained by applying a Taylor series expansion to the correlation coefficient

$$R_{uu}(\Delta y) = \frac{\overline{u(y+\Delta y)u(y)}}{\overline{u^2(y+\Delta y)}^{1/2}\,\overline{u^2(y)}^{1/2}} \quad (2)$$

R_{uu} was measured at five values of y^+. At each y^+, a range of values of Δy was used. The log–log plot in Figure 3a shows that for sufficiently small Δy^* [$\equiv \Delta y/\eta$, where η is the Kolmogorov length scale $\nu^{3/4}/\epsilon^{1/4}$ where ϵ is the mean energy dissipation rate approximated by its isotropic value $15\nu\overline{(\partial u/\partial x)^2}$] the data exhibit a +2 slope, a behaviour consistent with Equation 1. The upward trend at very small Δy^* ($\Delta y^* < 1$) is due mainly to the contribution from the electronic noise to $\overline{(\Delta u)^2}$ (Antonia et al. 1993). Using experimental estimates of $\overline{(\partial u^2/\partial y)^2}$ and the datapoints in Figure 3a which lie on the straight lines, Equation 1 was used to infer $\overline{(\partial u/\partial y)^2}$. Because this determination is relatively tedious, the values of $\overline{(\partial u/\partial y)^2}$ were used to calibrate $\overline{(\Delta u/\Delta y)^2}$. For various choices of Δy, the measured values of $\overline{(\Delta u/\Delta y)^2}$ were compared with the value of $\overline{(\partial u/\partial y)^2}$ inferred from Equation 1. Figure 3b shows that for each y^+, it is possible to identify a range of Δy^* over which $\overline{(\Delta u/\Delta y)^2}/\overline{(\partial u/\partial y)^2}$ is unity. On the basis of this result, it was possible to choose a particular (fixed) value of Δy so that Δy^* satisfied this requirement. For the riblet wall, Δy was 0.75 mm when $R_\theta = 540$ and 0.65 mm when $R_\theta = 940$. For the smooth plate, Δy was equal to 1.08 and 0.75 mm, respectively. The parallel wire probe with fixed Δy was subsequently traversed from the wall to $y^+ \simeq 100$ to provide a detailed variation of $\overline{(\partial u/\partial y)^2}$ in this part of the layer. By repeating each experiment at least twice, the uncertainty in $\overline{(\partial u/\partial y)^2}$ was estimated to be about 5%.

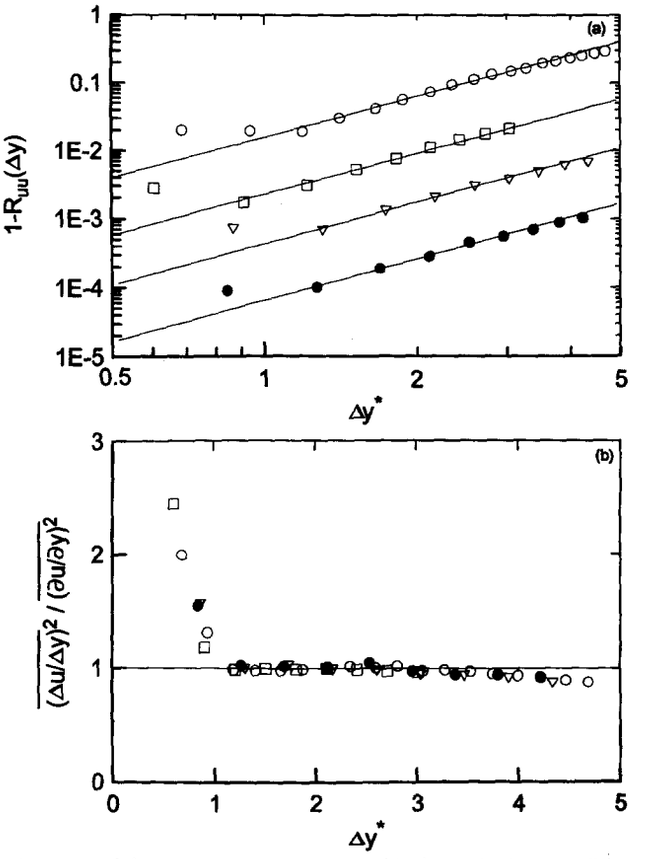

Figure 3 (a) log–log plot of $1 - R_{uu}(\Delta y)$ vs. Δy^* over riblet wall for $R_\theta = 540$; (b) $\overline{(\Delta u/\Delta y)'}/\overline{(\partial u/\partial y)}$ vs. Δy^* over a riblet wall; ○, $y^+ = 5$; □, 15; ▽, 24; ●, 40; lines have a slope of +2

Distributions of $(\partial u^+/\partial y^+)'$ are shown in Figure 4 for $y^+ \leq 100$ and the two values of R_θ. For the riblets, the data were obtained both over crest and valley. For the smooth wall, the results for $R_\theta = 540$ and $R_\theta = 940$ are in reasonable agreement with each other implying that there is no significant effect of R_θ on the wall normalised values of $(\partial u/\partial y)'$ in the wall region. Distributions for $(\partial u/\partial x)'$, not shown here, are almost identical at the two values of R_θ. Further support for this implication is our observation that the present smooth wall data of $(\partial u^+/\partial y^+)'$ are also in reasonable agreement with those, also in the wall region, previously reported by Balint et al. (1991) and Rajagopalan and Antonia (1993) at higher R_θ (2685 and 1450, respectively). It would appear that the noticeable low Reynolds number effects that have been observed for small scale turbulence statistics in the wall region of a fully developed channel flow (Antonia et al. 1991) are much less evident in the boundary layer. Indeed, the DNS rms vorticity data of Spalart (private communication, see also Antonia and Kim 1994) indicate that $\omega^{+'}$ and its components increase with R_θ only within the sublayer. The possibility that these may be genuine differences between the wall regions of the boundary layer and the channel flow would need to be carefully assessed, but this is beyond the scope of this paper. The important thing to note here is that $(\partial u^+/\partial y^+)'$ is reduced over the riblets, the reduction being more dramatic when the riblets operate in a roughness mode. It should, of course, be recalled that the smooth wall value of U_τ has been used to normalise the riblet data. A 5% reduction in U_τ would result in a 10% increase in $(\partial u^+/\partial y^+)'$ for $s^+ = 17$; this is clearly insufficient to account for the difference between the riblet data ($s^+ = 17$) and the smooth wall data, especially near the surface. For $s^+ = 29$, an increase in U_τ would mean an even bigger reduction in $(\partial u^+/\partial y^+)'$ than exhibited in Figure 4.

The reduction in $(\partial u^+/\partial y^+)'$ over the riblet valley (both $s^+ = 17$ and $s^+ = 29$) is consistent with the decrease in $\omega_z^{+'}$ reported by Choi et al. (1993) for $s^+ = 20$ and 40. There is no perceptible difference in the present data ($s^+ = 17$) between crest and valley except at $y^+ \leq 10$ when $(\partial u^+/\partial y^+)'$ over the crest dips below that over the valley; Choi et al. reported an increase over the crest relative to the valley for $s^+ = 20$. We could speculate that this discrepancy may reflect the need to have better spatial resolution over the crest than the valley (see end of previous section).

We can surmise that the reduction in $(\partial u^+/\partial y^+)'$ relative to a smooth wall reflects changes in the near-wall turbulence structure. The existence of intense internal shear layers extending up to $y^+ \simeq 100$ has been assumed to be important to the dynamics of the wall region under canonical conditions (e.g., Johansson et al. 1987a; Johansson et al. 1987b; Kline and Robinson 1989). The shear layers, which peel away from the wall at a relatively small inclination ($\simeq 10°$) to the surface, are characterised by high concentrations of $(\partial u/\partial x)'$, $(\partial u/\partial y)'$ and ω_z'. They delineate the interfaces between upstream high-speed fluid and downstream low-speed fluid and are often identified with the upstream side of lifted low-speed streaks (Robinson 1991). It seems plausible that the replacement of the flat wall by a grooved surface will tend to weaken the shear layers, the weakening becoming more pronounced as the Reynolds number increases; i.e., as the riblets become more roughness-like in behaviour. We would expect the eradication of the low-speed streaks as a fully rough behaviour is approached. It appears also likely that the weakening of the shear layers reflects in some way the changes to the vortices brought about by the different boundary conditions. Choi et al. (1993) presented visual evidence that the quasi-streamwise vortices are at a greater "effective" distance from the wall (relative to a smooth surface) when the riblets reduce the skin friction drag. In the limit of a fully rough wall layer, we would expect that the wall vortices are much less elongated in the streamwise direction than on the smooth wall case. Some evidence for this is provided by the data of Krogstad and Antonia (1994) for a k-type rough wall boundary layer; these data also indicated that the characteristic length scales in the x, y, z directions tended to be much more comparable than over a smooth wall. Correspondingly, the anisotropy of the Reynolds stress tensor is reduced over the roughness (Shafi and Antonia 1995). The present data for $(\partial u/\partial y)^2$ and $(\partial u/\partial x)^2$ [Taylor's hypothesis was used to estimate $(\partial u/\partial x)$] seem consistent with this. Indeed, the ratio $2\overline{(\partial u/\partial x)^2}/\overline{(\partial u/\partial y)^2}$ ($\equiv 1$ for isotropic turbulence) increases significantly (Figure 5), especially close to the wall, when the riblets are drag reducing. There is a further significant increase as R_θ is increased over the riblets (drag augmenting). This increased isotropy has been observed in the PIV data of Suzuki and Kasagi (1994).

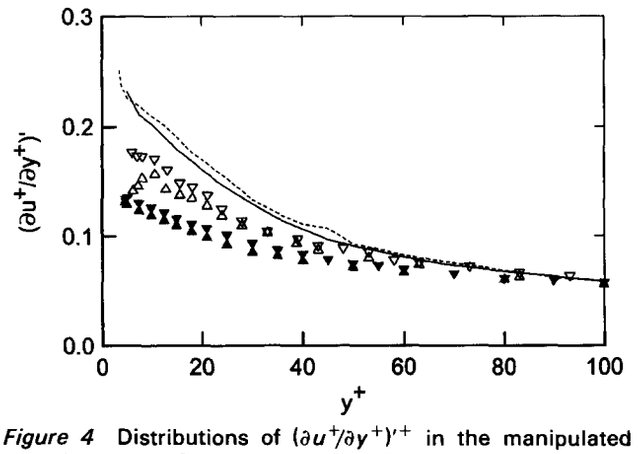

Figure 4 Distributions of $(\partial u^+/\partial y^+)'^+$ in the manipulated boundary layer; Symbols are as in Figure 2; Lines: smooth plate, —, $R_\theta = 940$; ---, $R_\theta = 540$

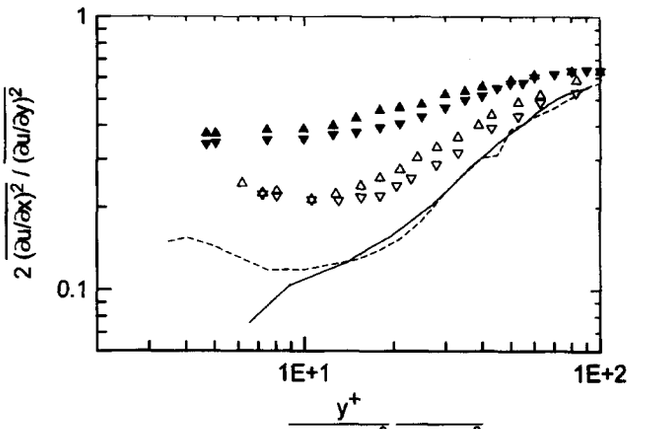

Figure 5 Distributions of $2\overline{(\partial u/\partial x)^2}/\overline{(\partial u/\partial y)^2}$; symbols are as for Figure 2; Lines: smooth plate, —, $R_\theta = 940$; --- $R_\theta = 540$

Conclusions

Statistics of $\partial u/\partial y$ have been measured in a turbulent boundary layer over either a smooth wall or a riblet surface. When the riblets are drag reducing, $(\partial u^+/\partial y^+)'$ is smaller than over a smooth wall, the difference increasing as the distance to the wall decreases. The difference is appreciably larger when the riblets are drag augmenting. One inference from the present results is that, relative to a smooth wall, the rms spanwise vorticity is

reduced near a riblet surface; the reduction should be larger when the riblets act as a rough wall. The present experimental results are in reasonable qualitative agreement with the DNS data of Choi et al. (1993), at least over the riblet valley. We speculate that the differences over the crest are due to the relatively poor spanwise spatial resolution of the hot wire measurements. The ratio $\overline{(\partial u/\partial y)^2}/\overline{(\partial u/\partial x)^2}$ is more isotropic over a riblet surface than on a smooth wall.

Acknowledgments

The support of the Australian Research Council is gratefully acknowledged.

References

Antonia, R. A. and Kim, J. 1994. Low Reynolds number effects on near-wall turbulence. *J. Fluid Mech.*, **276**, 61–80

Antonia, R. A., Kim, J. and Browne, L. W. B. 1991. Some characteristics of small-scale turbulence in a turbulent duct flow. *J. Fluid Mech.*, **233**, 369–388

Antonia, R. A., Zhu, Y. and Kim, J. 1993. On the measurement of lateral velocity derivatives in turbulent flows. *Exp. Fluids*, **15**, 65–69

Antonia, R. A., Zhu, Y. and Sokolov, M. 1995. Effect of concentrated wall suction on a turbulent boundary layer. *Phys. Fluids*, **7**, 2465–2474

Balint, J. -L., Wallace, J. M. and Vukoslavcevic, P. 1991. The velocity and vorticity vector fields of a turbulent boundary layer. Part 2, Velocity and vorticity vector fields of a turbulent boundary layer. Part 3, Statistical properties, *J. Fluid Mech.*, **228**, 53–86

Barenblatt, G. I. 1993. Scaling laws for fully developed turbulent shear flows. Part 1, Basic hypothesis and analysis. *J. Fluid Mech.*, **248**, 513–520

Barenblatt, G. I. and Prostokishin, V. M. 1993. Scaling laws for fully developed turbulent shear flows, Part 2. Processing of experimental data. *J. Fluid Mech.*, **248**, 521–529

Bechert, D. W. and Bartenwerfer, M. 1989. The viscous flow on surfaces with longitudinal ribs. *J. Fluid Mech.*, **206**, 105–129

Benhalilou, M., Anselmet, F. and Fulachier, L. 1994. Conditional Reynolds stress on a v-grooved surface. *Phys. Fluids*, **6**, 2101–2117

Choi, H., Moin, P. and Kim, J. 1993. Direct numerical simulation of turbulent flow over riblets. *J. Fluid Mech.*, **255**, 503–539

Djenidi, L. and Antonia, R. A. 1996. LDA measurements of a turbulent boundary layer over a riblets surface. *AIAA J.*, **34**, 1007–1012

Djenidi, L., Dubief, Y. and Antonia, R. A. 1996. Advantage of using a power law in a low R_θ turbulent boundary layer. *Exp. Fluids*, submitted

Johansson, A. V., Alfredsson, P. H. and Eckelmann, H. 1987a. On the evolution shear-layer structures in near-wall turbulence. In *Advances in Turbulence*, Springer-Verlag, Berlin, 383–390

Johansson, A. V., Alfredsson, P. H. and Kim, J. 1987b. Shear-layer structures in near-wall turbulence. *Proc. 1987 Summer Program Center for Turbulence Research*, Stanford University, Stanford, CA, 237–251

Kline, S. J. and Robinson, S. K. 1989. Quasi-coherent structures in the turbulent boundary layer. Part I, Status report on a community-wide summary of the data. In *Near-Wall Turbulence*, S. J. Kline and N. H. Afgan (eds.), Hemisphere, Bristol, PA, 200–217

Krogstad, P. -Å. and Antonia, R. A. 1994. Structure of turbulent boundary layers on smooth wall and rough walls. *J. Fluid Mech.*, **277**, 1–21

Park, S. Y. and Wallace, J. M. 1994. Flow alteration and drag reduction by riblets in a turbulent boundary layer. *AIAA J.*, **32**, 31–38

Rajagopalan, S. and Antonia, R. A. 1993. RMS spanwise vorticity measurements in a turbulent boundary layer. *Exp. Fluids*, **14**, 142–144

Robinson, S. K. 1991. Coherent motions in the turbulent boundary layer. *Ann. Rev. Fluid Mech.*, **23**, 601–639

Shafi, H. S. and Antonia, R. A. 1995. Anisotropy of the Reynolds stress in a turbulent boundary layer over a rough wall. *Exp. Fluids*, **18**, 213–215

Suzuki, Y. and Kasagi, N. 1994. Turbulent drag reduction mechanism above a riblet surface. *AIAA J.*, **32**, 1781–1790

Walsh, M. J. 1990. Riblets. In *Viscous Drag Reduction in Turbulent Boundary Layers*, Vol. 123, Progress in Astronautics and Aeronautics, D. M. Bushnell and J. N. Hefner (eds.), AIAA, New York, 203–261

Vukoslavcevic, P., Wallace, J. M. and Balint, J. -L. 1992. Viscous drag reduction using streamwise-aligned riblets. *AIAA J.* **30**, 1119–1122